Postprint of: Biernacki K. A., Kaczkowska E., Bruździak P., Aqueous solutions of NMA, Na_2HPO_4, and NaH_2PO_4 as models for interaction studies in phosphate–protein systems, Journal of Molecular Liquids, Vol. 265 (2018), pp. 361-371, DOI: 10.1016/j.molliq.2018.05.104

Aqueous solutions of NMA, Na_2HPO_4, and NaH_2PO_4 as models for interaction studies in phosphate–protein systems

Karol A. Biernacki, Emilia Kaczkowska, Piotr Bruździak[☆]

Department of Physical Chemistry, Gdańsk University of Technology, Narutowicza 11-12, 80-233 Gdańsk, Poland

Abstract

Phosphate buffers are essential for many areas of studies. However, their influence on buffered systems is often ignored. The phosphate salts can interact with biologically important macromolecules (e.g. proteins) and stabilize or destabilize them. With our research, we want to answer question what kind of interactions, if any, occur between phosphate ions and a protein backbone model – *N*–methylacetamide (NMA). ATR–FTIR spectroscopy in the amide I range and in the regions characteristic for P–O vibrations provides information on direct and indirect (water–mediated) interactions. The analysis is supported by chemometric, DFT, and QTAIM calculations. Our results indicate that direct NMA–phosphate ion interactions are quite rare and indirect. Water molecules seem to play an important role in such systems. The model studies indicate that no preferential interactions between NMA and phosphate ions in solutions are formed, and may imply that such interactions are also unfavorable in protein–based systems.

[☆]Corresponding author: *piotr.bruzdziak@pg.edu.pl*

Keywords: Phosphates, *N*-methylacetamide, Hydration, FTIR, DFT, QTAIM

1. Introduction

The constant pH of a solution is extremely important in many areas of chemistry, biology and physics. A simple way to stabilize it is to use buffers. Phosphate buffer is one of the most popular buffer in biological applications, composed of dihydrogen and hydrogen phosphate salts in various proportions. Its thermal stability and relatively wide physiological pH range (pH = $\pm$pK_a, i.e. 7.2$\pm$1.0) are advantageous in many protein-involving studies.[1] Phosphates are also essential building blocks of many biologically relevant molecules: DNA, RNA, phospholipid bilayers, ATP. The stability or energetics of various phosphate-related compounds makes these ions a perfect choice from the biological point of view.[2] Ideally, buffer constituents should not be able to interact with other components of the solution. Often the Pathak [3] effect of buffers on co-solutes is considered negligible, especially if their concentration is significantly higher than the buffer concentration (20-50 mM on average). However, even if the concentration is so low, some contacts occur and affects the type of interactions in the analyzed solutions,[4, 5, 6] especially if these solutions contain proteins or other macromolecules with concentrations usually a few orders of magnitude lower.

Recently, it has been proven that despite their low concentrations the ionized molecules of buffer components may also exert the Hofmeister effects on buffered macromolecules.[7, 8, 9] Thus, the electrochemical nature of a buffer must be taken into account when solutions are being prepared, not

only their optimal pH range. It is proven that buffer components can interact with polar and even non-polar fragments of a macromolecule through electrostatic or dispersive forces or influence their hydration.[10, 11, 12, 13] Such interactions can be either beneficial [14, 15, 16, 17, 18] or deleterious [19, 20, 21] and may affect not only thermal stability but many other properties of macromolecules.[9, 7] According to the classical Hofmeister series, HPO_4^{2-} ion can be considered as a kosmotropic agent, i.e. it orders water molecules in its surrounding. However, its water-structure-making properties not always explains the protein salting-out effect (and also its stability in solutions).[22, 23] Yet the idea of structure making or breaking can be misleading because enhancement or weakening of water interactions in hydration shells can occur simultaneously by a separation of hydration water population into distinct ordered and disordered sub-populations.[24] Despite the fact that the physiological role of phosphate ions is extremely important, their hydration is still poorly understood.[3, 25, 26, 27, 28, 29, 30]

This article is focused on the influence of the *N*–methylacetamide (NMA) molecule, which is often used as a minimal model compound of the protein backbone (a single peptide bond),[31, 32, 33, 34, 35, 36] on selected phosphate salts. NMA has been widely investigated in terms of its interactions with halide, alkali, and earth rare metals ions by means of many computational and experimental methods.[37, 33, 38, 39] The possibility of dimers and trimers formation of NMA molecules in solution has also been confirmed.[40, 41] Various clusters of NMA with protic and aprotic solvents has been described.[42, 43, 44, 45, 46] Time– or temperature–dependent changes in NMA solution structures, determined mainly by means of the vi-

brational spectroscopy, indicate that the structure of NMA oligomers closely resembles secondary structures of the protein backbone and in the presence of water undergoes a hydrophobic collapse similarly to more complex peptides.[47, 48] From a computational point of view, NMA is also an ideal minimal model for quantum mechanical calculations and molecular dynamics simulations concerning protein solvation. Such an approach has been recently applied to study interactions of NMA with various osmolytes and co-solutes, such as DMSO, TMAO, urea, tetramethylurea, and trehalose.[49, 50, 51] The choice of NMA as a model is also dictated by the greatest similarity, among other peptide bond imitating amides, of its hydration to the hydration of protein.[52] Therefore, the use of NMA molecule in presented studies appears to be justified.

2. Materials and Methods

2.1. Chemicals and Solutions

Dibasic sodium phosphate dihydrate ($Na_2HPO_4 \cdot 2H_2O$, 99%, Sigma-Aldrich), monohydrate monobasic sodium phosphate ($NaH_2PO_4 \cdot H_2O$, 99%, Sigma-Aldrich), NMA (99%, Aldrich), and deionized water (<0.01 $S \cdot cm^{-1}$), were used as supplied. For ATR–FTIR experimental section, ten solution series of Na_2HPO_4–NMA system were prepared. Concentration of Na_2HPO_4 was kept approximately constant in each series (0.0, 0.025, 0.05, 0.075, 0.1, 0.15, 0.25, 0.3, 0.4, 0.5 $mol \cdot dm^{-3}$, respectively). Each of the series consisted of seven different solutions in which concentration of NMA was increased (0.0, 0.5, 1.0, 2.0, 3.0, 4.0, 5.0 $mol \cdot dm^{-3}$, respectively). The same method was used to prepare six series of NaH_2PO_4–NMA water solutions, where con-

centration of NaH_2PO_4 was approximately equal (0.0, 0.2, 0.4, 0.6, 0.8, 1.0 mol·dm^{-3}, respectively), and each of this series consisted of eight solutions where concentrations of NMA were equal 0.0, 0.5, 1.0, 2.0, 3.0, 4.0, 5.0, 6.0 mol·dm^{-3}, respectively. Different concentration ranges were dictated by the differences in phosphate salts solubility. The concentrations of all chemicals were selected according to the demands of experimental technique. In most cases, the ATR–FTIR spectroscopy requires relatively high concentrations of solutes to obtain satisfactory spectra with low signal–to–noise ratio. Additionally, water absorption bands may obscure bands of other solution components, as in the case of NMA. However, as mentioned in paragraph 2.2.2, each concentration series was utilized to calculate derivatives or spectra in the infinite dilution approximation. Thus, all obtained spectra may be considered as corresponding to very diluted solutions.

All molar concentrations and molalities of NMA, water, and phosphate salts for the above-mentioned systems were calculated basing on appropriate weights of all components and densities of all prepared solutions, which were measured by means of a U–shaped tube densitometer (MG–2, UniLab, Poland). pH of each sample was measured with the Handylab pH-meter (Schott) equipped with a pH microelectrode. The average pH of samples containing Na_2HPO_4 or NaH_2PO_4 was equal to 9.21±0.21 or 4.50±0.35, respectively. Such values indicated that in those solutions only one form of phosphate ion was predominant (>97%).[25] Spectroscopic studies also confirmed that only one spectroscopic form of phosphate ions was present in each solution.

The bulk water spectrum was subtracted from each measured spectrum

with a subtracting factor calculated on the basis of molar concentration. That way, a grid of NMA–phosphate concentrations and corresponding spectra was created (i.e. a so-called three-way data set with four dimensions: wavenumber, NMA concentration, phosphate salt concentration, and absorbance). Due to the inevitable instrumental and preparation error, concentrations of all solution components in selected concentration dimension were not exactly equal. A fixed concentration of a spectral species in a grid line (i.e. a selected concentration dimension) is crucial for the next step of spectra analysis. Thus, the set of spectra was used for spectra interpolation to the grid of evenly spaced concentrations of NMA or phosphate ions using the Gridfit tool for Matlab by John R. D'Errico. The interpolation scheme was set to "bilinear" with a recommended smoothing factor of 1.

2.2. Methods of interaction studies in protein-osmolyte-water systems

2.2.1. ATR–FTIR spectroscopy

Spectra of all prepared solutions were recorded on Nicolet 8700 FTIR spectrometer (Thermo Scientific, Waltham, MA) equipped with an ATR accessory (6 internal reflections Ge crystal, Specac Ltd., Orpington, Great Britain). Temperature was kept at 25.0±0.1 ^{o}C using an electronic temperature controller (Specac Ltd., Orpington, Great Britain). Each recorded spectrum was obtained by measuring and averaging of 128 independent scans with 2 cm^{-1} resolution. The spectrometer was purged with dry nitrogen to minimize the influence of water vapor and carbon dioxide. All ATR–FTIR spectra were analyzed using commercial software: GRAMS/32 (Galactic Industries Corp., Salem, NH), OMNIC (Thermo Scientific, Waltham, MA), and Matlab (the MathWorks, Natic MA).

2.2.2. Difference spectra method

The difference spectra method applied in our research is based on the method proposed and developed by Stangret *et al.*[53, 54, 55, 56, 52] In general, the method allows to isolate the spectrum of an individual affected by some external factor (e.g. the presence of a co-solute, temperature, a change in concentration). The difference between the "bulk" (unaffected) spectrum and the one corresponding to the external change, i.e. a spectrum carrying all information about changes in such a system, can be added to the "bulk" spectrum with an appropriate coefficient. The coefficient carries information on the affected number, N, i.e. the number of moles of the analyzed individual perturbed by one mole (or one unit) of the affecting agent. However, the affected spectrum cannot be calculated if the affected number is unknown. The task of simultaneous determination of the number and affected spectrum is not trivial, and some ways to achieve the goal are presented in our previous papers.[57, 55]

Instead of a simple spectra difference calculation (where one spectrum corresponds to a unaffected species and the second one to the same species perturbed by an affecting agent or factor), a series of spectra with a fixed concentration of spectral species of interest is measured. In each spectrum of the series the molality, m_a, of an affecting agent (or factor) varies. From such a series for each wavenumber a derivative of absorbance vs. m_a is then calculated. The derivative at $m_a = 0$ (i.e. the extrapolation of the change in absorbance to the infinite dilution of the affecting agent):

$$D_\nu = \left(\frac{\partial A_\nu}{\partial m}\right)_{m\to 0}$$

gives an information on changes caused by the introduction of affecting agent,

similarly to a simple difference spectrum. Such a derivative is calculated for each wavelength, (we will denote it as D), thus a set of all calculated derivative values has a spectrum-like nature. In fact, its shape contains only the information on changes in the spectral shape of analyzed species of interest caused by the introduction of affecting agent or factor.

2.2.3. DFT and QTAIM calculations

DFT calculations of simple NMA–H_2O–phosphate ion systems were performed according to the scheme presented in our previous paper.[24] The final structures and frequencies were calculated with the M06-2X density functional method,[58] the aug-cc-pVTZ basis set,[59] and the conductor-like polarizable continuum model (CPCM), with water set as the solvent.[60, 61] The basis set superposition errors of energies (BSSE) were calculated for the final CPCM-optimized geometries using the counterpoise method.[62] Such a scheme of calculations allowed us in our previous paper to reproduce and interpret changes in the frequencies of vibration of simple complexes to a satisfactory degree.[24] In order to compare the energy values of hydrogen bonds, the energies of simple water clusters composed of up to 4 molecules of water were also calculated.

In our research, almost only the *trans* form of NMA was taken into consideration. In aqueous solution, the *trans* conformation is much more probable, as confirmed by experimental results and theoretical calculations.[63, 64, 65] Moreover, it reflects better the conformation of the protein backbone.

Due to a significantly large number of atoms, the geometry optimizations of hydrated complexes were performed only in the gas phase using the same method, but with a smaller basis set – cc-pVTZ. Electron densities of such

large systems, calculated for the optimized final structures, were next analyzed according to the Quantum Theory of Atoms In Molecules (QTAIM).[66] Energies of selected hydrogen bonds were estimated [67] on the basis of the potential energy density, V_r, at the bond critical points between hydrogen atom and its acceptor:

$$E_{HB} = \frac{1}{2} V_r$$

However, the calculated E_{HB} values were used only for comparison between various systems.

The optimization and frequency calculation steps were performed with the Gaussian 09v.D1 (Gaussian Inc., Wallingford, CT) software [68] available at the Academic Computer Center in Gdansk (TASK), analyzed and visualized with Avogadro software v.1.1.1.[69] Calculations within the QTAIM theory were performed with the Multiwfn software v. 3.3.9.[70]

3. Results and Discussion

3.1. Initial remarks

In our initial remarks we need to justify measurements and analysis of spectral series of NMA (or phosphate ions) affected only by its concentration (i.e. in such systems only NMA, or phosphate ions, and water are present). Changes in such spectral series are characteristic only for direct or indirect interaction between the same kind of molecules. Such interactions have to be taken into account in ternary systems (i.e. NMA–water–phosphate ion) because the presence of an additional solution component may promote concentration–dependent structural changes of the analyzed molecule. The

addition of the third component of the solution causes decrease in water concentration, and even if the concentration of the first main component (here NMA) is constant with and without the third compound, the amount of accessible water molecules must be lower. However, in the case of our systems such an effect turned out to be negligible and no concentration–dependent changes in ternary systems were observed for any of analyzed components (NMA, $H_2PO_4^-$, HPO_4^{2-}).

Because most of the changes in the analyzed systems in the following paragraphs are very small and may not be easily visible even in the so-called affected spectra, some of them will be indicated in the derivative D, which carries all information about changes in the spectral series. The sense of the derivative is discussed in paragraph 2.2.2.

3.2. Changes in the shape of NMA spectra of pure NMA solutions

Spectra of NMA affected by changes in its concentration were measured in both analyzed systems of phosphate ions. Changes in such spectral series were identical.

Molar ATR–FTIR spectra of NMA in aqueous solutions corresponding to different NMA concentrations are shown in Figure 1a. The bulk water spectrum was subtracted from each of them with an appropriate subtraction factor. The maximum of the peak at ca. 1625 cm^{-1}, assigned to the stretching vibration of C=O bond, significantly shifts towards higher wavenumbers, along with the increase of NMA concentration. Changes in the position of the band corresponding to the bending vibration of N–H bond, with maximum at ca. 1580 cm^{-1}, are barely visible, because it is obscured by a stronger C=O band. Any shift in its position is below the measurement resolution.

Thus, it should be concluded that this band does not change its position. The confirmation of this two above-mentioned statements can be found in the shape of the derivative (Figure 1b) for changes of NMA caused by its increased concentration. The characteristic shape indicates a strong shift towards higher wavenumber values of a single band in the amide I region. Most importantly, there is no change of the band shape contour at the N–H bond region. However, DFT calculation clearly indicate that the change in C=O bond of NMA, being a result of interaction with another molecule, has to have an influence on the N–H bond in peptide moiety, and *vice versa*. For example, in a complex of two molecules of NMA (Figure 2e), theoretical calculations predict that bands corresponding to the stretching vibration of C=O bond and bending vibration of N–H bond split into two low– and high–wavenumber components (Table 2).

The chemometric analysis of the spectra series clarified the picture. From the concentration–affected NMA spectra three principal factors could be extracted (Figure 1a). The Malinowski‘s spectral isolation factor analysis algorithm [71, 72] allowed to estimate band shapes of those three factors. Two of them closely resembled the NMA bulk spectrum and revealed the missing shift in the N–H band position, hidden in the series of spectra and in the derivative *D*. In one of those factors both peaks (C=O stretching and N–H bending) are relatively close to each other, while in the second one both of them are clearly separated and shifted in directions predicted by DFT calculations. As expected, these two factors exchange their relative concentrations in the spectral series (Figure 1c). Although both factors are abstract mathematical representations of the gradual shifts in the spectra series, they

allow to conclude that observed changes were results of direct NMA–NMA interactions in solution. The third isolated principal factor is similar to a difference spectrum and can be simply a correction due to the change in the C=O band intensity.

In conclusion, ATR–FTIR studies indicate that NMA in aqueous solutions can form higher–order structures in the given concentration, relatively wide, range. Theoretical calculations confirm these observations. Other reports confirm such finding, although such interactions are thought to be weak.[73, 74]

3.3. NMA in the presence of phosphate ions

The shape and character of changes in the derivatives D of phosphate-affected NMA in both considered systems were similar to the changes of bands corresponding to bending vibrations of water molecules affected by phosphate ions. This indicated that the main changes observed in these derivatives were not caused by the phosphate-affected vibrational structure of NMA. Most of the observed changes came from the water disordered by the presence of phosphate ions. Thus, there was no need to isolate the spectra of NMA affected by presence of phosphates, because with the given spectral resolution and experimental error no changes in NMA structure could be indicated and it could be even misleading. Summarizing, the vibrational structure of NMA was generally not affected by interactions with phosphate ions.

3.4. Changes in the band shape of $H_2PO_4^-$ ion spectrum caused by an increase of its concentration

The ATR–FTIR molar spectra of $H_2PO_4^-$ ion in the P–O vibration range affected by changes in its concentration are shown in Figure 3a. The bulk water spectrum was subtracted from all the spectra with a subtraction factor calculated according to the water molar concentration. The peak at ca. 1160 cm^{-1}, which can be attributed to the asymmetric stretching vibrations of P–O bond,[75] slightly shifts to lower wavenumbers along with the increase of $H_2PO_4^-$ concentration. There is no visible change in the band position of symmetric stretching P–O vibration band at ca. 1075 cm^{-1},[75] except for the change of its intensity. However, the shape of derivative in this region suggests that the band increases its width and slightly shifts towards lower wavenumbers. The blue shift of the peak at ca. 940 cm^{-1}, which can be attributed to asymmetric stretching vibrations of P–OH bonds, is smaller than the resolution of measurement, but the shape of the difference derivative spectrum (Figure 3c) in the region of P–OH stretching vibrations suggests, that the difference between spectra is meaningful.

The DFT calculations indicate that the complex of two $H_2PO_4^-$ ions, binding each other with three hydrogen bonds (Figure 2j), is even more favorable than the complex of the same phosphate anion and water molecule (Table 1). The calculations predict the direction of changes in the wavenumbers of all considered bonds of $H_2PO_4^-$ ion (Table 2) in such a complex. Thus, it is possible that $H_2PO_4^-$ ions create dimers in aqueous solution.

Observed changes are getting stronger with the increase of concentration, mostly because the probability to interact two ions in solution is higher. The

	E(el.+ZPC)[a]	BSSE[b]	ΔE[c]	HB[d]	E_{HB}[e]
	hartree	kJ·mol^{-1}	kJ·mol^{-1}		kJ·mol^{-1}
Water (H_2O)	-76.415493	–	–	–	–
$(H_2O)_2$	-152.834425	0.3	-8.8	1	-8.8
$(H_2O)_3$	-229.255430	0.9	-22.6	3	-7.5
$(H_2O)_4$	-305.680529	1.6	-47.2	4	-11.8
a) *cis*–NMA	-248.417519	–	–	–	–
b) *trans*–NMA	-248.420800	–	–	–	–
c) $H_2PO_4^-$	-643.742814	–	–	–	–
d) HPO_4^{2-}	-643.269087	–	–	–	–
e) NMA–NMA	-496.849311	1.2	-19.1	1	-19.1
f) $NMA_{(N-H)}$–H_2O	-324.840363	0.6	-10.1	1	-10.1
g) $NMA_{(C=O)}$–H_2O	-324.842722	0.5	-16.3	1	-16.3
h) NMA–$H_2PO_4^-$	-892.173602	1.4	-24.9	1	-24.9
i) NMA–HPO_4^{2-}	-891.704366	1.5	-36.5	1	-36.5
j) $H_2PO_4^-$–$H_2PO_4^-$	-1287.517235	2.6	-80.4	3	-26.8
k) $H_2PO_4^-$–H_2O	-720.167828	0.8	-24.2	2	-12.1
l) HPO_4^{2-}–H_2O	-719.699748	0.9	-39.0	2	-19.5
m) NMA–H_2O–$H_2PO_4^-$	-968.598946	2.1	-50.1	3	-16.7
n) NMA[f]–HPO_4^{2-}–H_2O	-968.127854	2.5	-65.1	2	-32.5

Table 1: Results of DFT (M06-2X/aug-cc-pVTZ, CPCM) energy calculations for various complexes of water, NMA, $H_2PO_4^-$, and HPO_4^{2-}.[a] Sum of electronic and zero point energies, [b] basis set superposition error, [c] energy of interaction (BSSE included), [d] number of excessive hydrogen bonds in a complex, [e] energy of interaction per one excessive hydrogen bond, [f] geometry optimization of such a complex possible only for the *cis* form of NMA; all other complexes were optimized with the *trans* form. Lower letters next to the types of complexes correspond to Figure 2.

Experimental frequencies					
	ν_{as} P–OH	ν_{s} P–O	ν_{as} P–O	νC=O	δN–H
NMA	–	–	–	1621	1579
$H_2PO_4^-$	943	1078	1160	–	–
HPO_4^{2-}	–	990	1080	–	–
Results of frequency calculation for various complexes					
	ν_{as} P–OH	ν_{s} P–O	ν_{as} P–O	νC=O	δN–H
a) *cis*–NMA	–	–	–	1703	1525
b) *trans*–NMA	–	–	–	1710	1569
c) $H_2PO_4^-$	837	1109	1280	–	–
d) HPO_4^{2-}	–	978	1136	–	–
e) NMA–NMA	–	–	–	$1691^a/1706^b$	$1610^a/1581^b$
f) $NMA_{(N-H)}$–H_2O	–	–	–	1703	1595
g) $NMA_{(C=O)}$–H_2O	–	–	–	1690	1584
h) NMA–$H_2PO_4^-$	851	1108	1270	1695	1618
i) NMA–HPO_4^{2-}	–	998	1094	1681	1641
j) $H_2PO_4^-$–$H_2PO_4^-$	927	1106	1230	–	–
k) $H_2PO_4^-$–H_2O	857	1107	1262	–	–
l) HPO_4^{2-}–H_2O	–	973	1149/1084	–	–
m) NMA–H_2O–$H_2PO_4^-$	869	1087	1214	1689	1588
n) NMA^*–HPO_4^{2-}–H_2O	–	975	1078/1165	1692	1559

Table 2: Results of DFT (M06-2X/aug-cc-pVTZ, CPCM) frequency calculations for various complexes of NMA, $H_2PO_4^-$, and HPO_4^{2-}. All complexes containing NMA were calculated with the *trans* isomer of the compound. ^{a} A group engaged in the HB formation; ^{b} free group. * Geometry optimization of such a complex possible only for *cis* form of NMA; all other complexes were optimized with the *trans* form. Lower letters next to the types of complexes correspond to Figure 2.

formation of $H_2PO_4^-$ dimers in aqueous solutions has been confirmed in other works.[76, 77, 78]

3.5. Changes in the shape of $H_2PO_4^-$ ion spectra caused by the presence of NMA

The changes in the peak shapes at ca. 1160 cm^{-1} and ca. 1075 cm^{-1} (Figure 3b) are caused by presence of NMA. The maximum of the spectra responsible for asymmetric stretching vibrations of P–OH bond and asymmetric stretching vibrations of P–O bond changing towards lower wavenumber values. The differences are much more evident than those observed in the case of $H_2PO_4^-$ spectra caused by the increase of its concentration. This suggests that $H_2PO_4^-$ ions are affected to some extent by the presence of NMA. Differences in the shape of the derivatives for this NMA–affected series, and the previous one, caused only by the change in its concentration, supports the statement (Figure 3c).

The number of ions affected by NMA (Table 3) is very low (N=0.01–0.15) indicating that such interactions are no numerous, yet its higher than in the case of the second phosphate ion. Additionally, the affected number is roughly proportional to the increase of $H_2PO_4^-$ ion concentration suggesting that such weak interactions are not preferentially created or inhibited in a solution.

The DFT calculations of simple complexes indicate that the structure consisting of NMA molecule and $H_2PO_4^-$ ion mediated by one water molecule (Figure 2m) is favorable (Table 1). The results of calculations also predict the direction of shifts in wavenumbers (Table 2) for this kind of structure. Thus, it is likely that in such systems indirect interactions through water

$[H_2PO_4^-]$ mol·dm^{-3}	N	$[HPO_4^{2-}]$ mol·dm^{-3}	N
0.1104	0.02	0.0477	0.01
0.2209	0.05	0.0954	0.02
0.3313	0.07	0.1431	0.02
0.4417	0.09	0.1908	0.03
0.5521	0.10	0.2385	0.03
0.6626	0.12	0.3339	0.01
0.7730	0.13	–	–
0.8834	0.15	–	–

Table 3: Affected numbers, N, denoting the number of phosphate ion moles affected by one mole of NMA, determined for systems in which phosphate ion concentration was kept constant in a series and NMA concentration varied.

molecules are preferred.

In sum, DFT calculations indicate, that it is possible for dimers of $H_2PO_4^-$ to occur in aqueous solution of NaH_2PO_4. The interaction energy (Table 1) for this structure is more favorable than for complex consist of NMA-H_2O-$H_2PO_4^-$. However, a structure composed of NMA, H_2O and $H_2PO_4^-$ molecules is also favorable in aqueous solution, which is confirmed by changing in spectra of $H_2PO_4^-$ caused by presence of NMA. Finally, the most proper assumption is that both of mentioned forms are present in aqueous solution

3.6. Changes in the band shape of HPO_4^{2-} ion spectrum caused by the increase of its concentration

The changes in ATR–FTIR spectra caused by the increase of HPO_4^{2-} concentration are shown in Figure 4a. Peaks at ca. 1080 cm^{-1} and at ca. 990 cm^{-1} can be assigned to the asymmetric stretching vibration of P–O bond and the symmetric stretching vibration of P–O bond, respectively.[75] No changes in the band shape for these two regions are visible. Therefore, HPO_4^{2-} ions in aqueous solution do not interact with each other or do not exert any significant influence on neighboring anions in the given concentration range. Confirmation of these statements is given in the shape of the derivative D (Figure 4c) which is very noisy and does not indicate any significant changes in the considered spectral region. The simplest explanation of this behavior is the high electrostatic charge of HPO_4^{2-} ions, which causes their repulsion in aqueous solution. It was impossible to finish the optimization step of DFT calculations scheme for the complex consisting of two HPO_4^{2-} molecules, because the distance between this two ion was constantly increasing. Thus, in contrast to $H_2PO_4^-$, HPO_4^{2-} ions do not form dimers in aqueous solution, at least not in the analyzed concentration range.

3.7. Changes in the shape of HPO_4^{2-} ion spectra caused by presence of NMA

Spectra of HPO_4^{2-} ion affected by the presence of NMA are shown in Figure 4b. The maxima of peaks in the regions responsible for asymmetric stretching vibrations of P–O bond and symmetric stretching vibrations of P–O bond shift towards lower wavenumbers. This suggests that HPO_4^{2-} ions are affected by the presence of NMA in solution. However, the shape of the derivative D in NMA–affected spectra series of HPO_4^{2-} ion (Figure

4c) is similar to spectra of HPO_4^{2-} in this series. It means, that changes in the vibrational structure of HPO_4^{2-} ion being a result of interaction between HPO_4^{2-} and NMA molecules are very weak and non specific.[79]

DFT calculations suggest that a simple structure consisting of NMA and HPO_4^{2-} ion (Figure 2i) is favorable in aqueous solution (Table 1), However, such a structure does not take into account the presence of water molecules. It was impossible to optimize geometry of a simple complex of NMA, water molecule, and the phosphate ion in the same manner as in the case of NMA–H_2O–$H_2PO_4^-$. A strong interaction (Table 1) between NMA and HPO_4^{2-} was formed with the water molecule attached on the other side of the ion (Figure 2n). In a real solution, NMA in such a complex should exhibit a visible shifts in its spectra (Table 2), however, in reality NMA molecules are not affected significantly in the solution of HPO_4^{2-}. Thus, we can conclude that such a complex in not likely to be present in solutions. Moreover, the value of affected number (Table 3), which denotes the number of moles of the HPO_4^{2-} affected by 1 mole of NMA molecules, is extremely low (N=0.01–0.03). Moreover, there is no visible correlation between its value and HPO_4^{2-} concentration. This all may suggest that such interactions are inhibited even at higher concentrations. Again, it indicates that interactions between HPO_4^{2-} ion and NMA molecule are strictly limited and are of indirect nature.

3.8. DFT calculations of hydrated phosphate-NMA complexes

Because ATR–FTIR results clearly indicated that NMA–phosphate ions interactions are limited in a solution and that direct interactions between them are not likely to be possible, we focused on the hydration shell of phosphate ions as a possible source of observed changes in phosphate ions

spectra.

A successful attempt to simulate the influence of NMA on the minimal hydration shell of the selected phosphate ions was made. The shell in both cases consisted of 13 water molecules to satisfy all hydrogen bond donor and acceptor sites of phosphate ions. NMA molecule, with its minimal number of affected water molecules N=3,[52] was placed in the surrounding of the phosphate hydration shell in a tangent plane facing phosphate oxygen atom with the tangent point placed approximately between nitrogen and carbon of carbonyl group of NMA. That way, four complexes, corresponding to four oxygen atoms of phosphate ions, were created for each phosphate-NMA pair and their structures were optimized.

In none of these complexes direct NMA–phosphate ion interactions were formed. In all cases, NMA kept its water molecules and in almost every case the NMA–3H_2O complex oriented itself perpendicularly to its initial orientation. In Figure 5 only two selected structures are presented. Due to the size of figures and the same most important features, all other structures are presented in Supplementary Materials. In the $H_2PO_4^-$–based systems, a water molecule bridging the N–H bond and the phosphate hydration shell was not incorporated into the hydration layer of $H_2PO_4^-$ in none of the optimized complexes (Figure 5a), while in the case of HPO_4^{2-} the molecule was forced in two cases to interact directly with the phosphate ion, reshaping its hydration shell (Figure 5b). We calculated oxygen-oxygen distances of water molecules in hydration shells, R_{OO}, of both ions for all those systems (Figure 6). Results indicate that although water molecules around $H_2PO_4^-$ ion are on average marginally affected by the presence of NMA yet some

of R_{OO} distances are shortened, which can be a sign of an enhancement of water structure in such a binary system. In the case of HPO_4^{2-} the R_{OO} distances were significantly larger when NMA was introduced to the system. Such a result could suggest that the hydration shell had swelled and possibly phosphate–water interactions had weakened. Instead, spectroscopic results suggested that interactions between oxygen atoms of HPO_4^{2-} ion and water molecules had strengthened (the PO stretching vibration bands shifted towards lower wavenumbers). While results for $H_2PO_4^-$–water–NMA system stay in a good agreement with experimental ones, DFT calculations of HPO_4^{2-}–water–NMA system do not validate clearly experimental observations. A more reliable picture of interaction emerges from the results of the QTAIM calculations and the analysis of energies at specific points in space between atoms, called critical points.

3.9. QTAIM calculations

Electron densities of aqueous complexes, a "by-product" of DFT calculations, were subjected to the analysis according to the QTAIM theory. The hydrogen bond energy between donor an acceptor is proportional to the potential electron density, V_r, at the critical point between proton and its acceptor [67] and can be used to estimate the influence of an external factor on its changes. Results of the calculations of both types of complexes (HPO_4^{2-}– and $H_2PO_4^-$–based) indicate that the presence of NMA with its three water molecules influences differently the mean hydrogen bond energy between oxygen atoms of phosphate ion and surrounding molecules (Table 4). The mean HB energy gain is larger in the case of HPO_4^{2-} (-67.3 kJ), however, the energy is dispersed over a larger number of such interaction, as one

	HPO_4^{2-}·13H_2O [a]	+NMA·3H_2O O1 [b]		+NMA·3H_2O O2 [b]		+NMA·3H_2O O3 [b]		+NMA·3H_2O O4 [b]		Mean (O1–O4) [c]	
ΣE_{HB} [d]	-446.1	-487.1	-41	-587.4	-141.3	-485.3	-39.2	-494.1	-48	-513.4	-67.3
N_{CP} [e]	13	15		12		14		13		13.5	
$\overline{E}_{HB}$ [f]	-34.3	-32.5	1.8	-48.9	-14.6	-34.7	-0.3	-38	-3.7	-38.5	-4.2
$\overline{E}_{HB}$(O1) [g]	-20.5	-23.5	-3	-22.4	-1.9	-16.8	3.8	-21.5	-0.9	-21	-0.5
$\overline{E}_{HB}$(O1H) [h]	-31.7	-48.4	-16.7	-69.7	-38	-22.3	9.4	-41.4	-9.7	-45.5	-13.7
$\overline{E}_{HB}$(O2) [g]	-37.6	-31.5	6.1	-51.3	-13.7	-35.7	1.9	-36.8	0.8	-38.8	-1.2
$\overline{E}_{HB}$(O3) [g]	-43	-33.9	9.1	-45.7	-2.7	-56.9	-13.9	-43.3	-0.3	-45	-1.9
$\overline{E}_{HB}$(O4) [g]	-32.9	-32.5	0.4	-60.7	-27.8	-33.7	-0.8	-42.3	-9.5	-42.3	-9.4
	$H_2PO_4^-$·13H2O [a]	+NMA·3H_2O O1 [b]		+NMA·3H_2O O2 [b]		+NMA·3H_2O O3 [b]		+NMA·3H_2O O4 [b]		Mean (O1–O4) [c]	
ΣE_{HB} [d]	-486.6	-497.3	-10.6	-534.9	-48.3	-548.7	-62.1	-489	-2.4	-517.5	-30.8
N_{CP} [e]	13	12		12		12		12		12	
$\overline{E}_{HB}$ [f]	-37.4	-41.4	-4	-44.6	-7.1	-45.7	-8.3	-40.8	-3.3	-43.1	-5.7
$\overline{E}_{HB}$(O1) [g]	-16.8	-20.5	-3.6	-17	-0.1	-18.3	-1.4	-16.3	0.6	-18	-1.2
$\overline{E}_{HB}$(O1H) [h]	-75	-85.2	-10.2	-91.9	-16.9	-99.4	-24.4	-80.4	-5.3	-89.2	-14.2
$\overline{E}_{HB}$(O2) [g]	-20.4	-19.2	1.1	-22.6	-2.3	-18.3	2.1	-16	4.4	-19	1.3
$\overline{E}_{HB}$(O2H) [h]	-104	-107.6	-3.6	-106.7	-2.7	-106.2	-2.2	-104.7	-0.7	-106.3	-2.3
$\overline{E}_{HB}$(O3) [g]	-27.6	-28.3	-0.7	-38.4	-10.8	-41.1	-13.5	-30.2	-2.6	-34.5	-6.9
$\overline{E}_{HB}$(O4) [g]	-37.6	-46.7	-9.1	-47.3	-9.6	-49	-11.4	-49.6	-12	-48.1	-10.5

Table 4: Energies of PO···HOH or POH···OH_2 hydrogen bonds in various phosphate–NMA complexes, calculated within the QTAIM theory. All energies are given in kJ·mol^{-1}. Labels of oxygen atoms are as in Figure 2. [a] A system composed of phosphate ion and 13 water molecules. [b] A system composed of hydrated phosphate ion (13 water molecules) and NMA·3H_2O; the center of NMA molecule was oriented near the O1, O2, O3 or O4 phosphate oxygen in the initial structures, respectively; the second column gives the differences between the given energies and corresponding energies in the ion·13H_2O complex. [c] Mean values of energies of O1 – O4 systems. [d] The sum of all energies of hydrogen bonds between water molecules and phosphate oxygen atoms or OH groups at bonding critical points. [e] The number of bonding critical points of such hydrogen bonds found in complex structures. [f] The mean hydrogen bond energy. [g] The mean energy of hydrogen bond involving a given phosphate oxygen atom of phosphate ion. [h] The mean energy of hydrogen bond involving a given OH group of phosphate ion.

additional water molecule of NMA is incorporated into the hydration shell of the ion. Thus, the mean energy gain for a single hydrogen bond is larger for the $H_2PO_4^-$–based system (-5.7 kJ) in comparison to the HPO_4^{2-}–based (-4.2 kJ), for which the number of HB interaction is even lower when the NMA molecules is approached, according to the number of critical points found. Therefore, the interactions between phosphate ions and water molecules in the presence of NMA is enhanced in both cases, though the need for reshaping of the hydration layer of the HPO_4^{2-} ion diminishes the energetic gain. Additionally, if $HPO_4^{2-}\cdots H_2O$ hydrogen bond energies are higher, the P–O stretching vibrations should lower their frequencies (as seen in experimental spectra), even though the DFT–based geometric parameters indicate larger R_{OO} distances between hydration water molecules.

The QTAIM analysis clearly indicates that O–H bond of phosphate ions is the most sensitive bond for any changes in the hydration layer. The $POH\cdots OH_2$ hydrogen bonds experiences much larger change in such complexes than the $PO\cdots HOH$ ones, and its share in the overall energetic gain is the largest. Such a bond is obviously more numerous in the case of $H_2PO_4^-$ ion, hence the lower mean energies of hydrogen bonds in such a case.

We can conclude that in our case the QTAIM–supported analysis of DFT calculations gives a better and more reliable picture of interactions in solutions.

4. Conclusions

The results of FTIR studies, supported by DFT calculations of simple complexes, indicates that in pure solutions of HPO_4^{2-} no dimers or higher

order aggregates are formed up to the concentrations selected for this work. In contrast, $H_2PO_4^-$ ions may interact with each other in aqueous solutions, although such interactions are quite weak and not numerous at selected concentration range, as indicated by low affected number values, *N*. Similarly, oligomers of NMA can be formed in its aqueous solutions.

In ternary NMA–water–phosphate ion solutions new types of interactions are present. Both $H_2PO_4^-$ and HPO_4^{2-} ions react to the presence of NMA molecule with changes in their spectral band shapes of the PO vibration region. However, both experimental results and theoretical calculations suggest that such interactions are of indirect manner. This conclusion is supported by the lack of any significant changes in the band shape of NMA in phosphate solutions. All changes in the amide I region of this molecules can be ascribed to the changes in the shape of the O–H water bending vibration band. The simplest explanation is that both phosphate and NMA molecules interact through their hydration shells and such a type of interaction affects mostly phosphate ions, not NMA. The fact that these compounds react differently may be hidden in the differences in their hydration. Water molecules in hydration shells of both phosphate ions is highly organized in comparison to the bulk water,[25] and to the water affected by NMA.[52]

In our discussion we omit the influence of Na^+. However, our results indicate that in such systems only the phosphate part is significantly affected, not NMA. Thus, any interaction of the latter with sodium ion are not visible with selected experimental method and is such a case it can be regarded as negligible.

In the context of phosphate-protein backbone interactions, our results

may indicate that phosphate ions are excluded from the protein backbone surrounding (indirect character of interactions, low N numbers). In simple systems, such an approaching of the phosphate ions to the protein's hydration shell would be unfavorable and promote backbone exclusion from the phosphate surrounding (and vice versa). Without other factors such interactions would be beneficial for protein stability. However, the disruption of highly organized hydration shell of phosphate ions could be paid for with other types of interaction, e.g. electrostatic interactions with positively charge residues at the protein surface. In this context, the choice of NMA as the model of protein backbone may be too simplistic and insufficient. Further studies are needed involving other more sophisticated models of polypeptide backbone, possibly with charged groups introducing the possibility of electrostatic interactions. Future works may also include other buffers with pH close to 7.0 or phosphate salts with different counterions to help understand the role of buffers and their composition on ion specific phenomena involving protein stability in solutions.

5. Acknowledgements

This research was supported by the Academic Computer Center in Gdansk (CI TASK).

6. Declaration of interest

The authors declare that they have no conflict of interest.

7. References

[1] P. Kolhe, E. Amend, S. K. Singh, Impact of freezing on pH of buffered solutions and consequences for monoclonal antibody aggregation, Biotechnology Progress 26 (2010) 727–733.

[2] F. Westheimer, Why nature chose phosphates, Science 235 (1987) 1173–1178.

[3] A. K. Pathak, Stepwise hydration of phosphate anion: A microscopic theory connecting domain of instability and stability, International Journal of Quantum Chemistry 115 (2015) 413–418.

[4] Y. R. Gokarn, R. M. Fesinmeyer, A. Saluja, V. Razinkov, S. F. Chase, T. M. Laue, D. N. Brems, Effective charge measurements reveal selective and preferential accumulation of anions, but not cations, at the protein surface in dilute salt solutions, Protein Science 20 (2011) 580–587.

[5] L. Medda, C. Carucci, D. F. Parsons, B. W. Ninham, M. Monduzzi, A. Salis, Specific cation effects on hemoglobin aggregation below and at physiological salt concentration, Langmuir 29 (2013) 15350–15358.

[6] J. M. Borah, S. Mahiuddin, N. Sarma, D. F. Parsons, B. W. Ninham, Specific ion effects on adsorption at the solid/electrolyte interface: A probe into the concentration limit, Langmuir 27 (2011) 8710–8717.

[7] F. Cugia, S. Sedda, F. Pitzalis, D. F. Parsons, M. Monduzzi, A. Salis, Are specific buffer effects the new frontier of Hofmeister phenomena? Insights from lysozyme adsorption on ordered mesoporous silica, RSC Advances 6 (2016) 94617–94621.

[8] L. Medda, M. Monduzzi, A. Salis, The molecular motion of bovine serum albumin under physiological conditions is ion specific, Chem. Commun. 51 (2015) 6663–6666.

[9] F. Cugia, M. Monduzzi, B. W. Ninham, A. Salis, Interplay of ion specificity, pH and buffers: insights from electrophoretic mobility and pH measurements of lysozyme solutions, RSC Advances 3 (2013) 5882.

[10] D. Parsons, M. Boström, P. Lo Nostro, B. Ninham, Hofmeister effects: interplay of hydration, nonelectrostatic potentials, and ion size, Physical Chemistry Chemical Physics 13 (2011) 12352–12367.

[11] S. Ohtake, Y. Kita, T. Arakawa, Interactions of formulation excipients with proteins in solution and in the dried state, Advanced Drug Delivery Reviews 63 (2011) 1053–1073.

[12] T. J. Zbacnik, R. E. Holcomb, D. S. Katayama, B. M. Murphy, R. W. Payne, R. C. Coccaro, G. J. Evans, J. E. Matsuura, C. S. Henry, M. C. Manning, Role of Buffers in Protein Formulations, Journal of Pharmaceutical Sciences 106 (2017) 713–733.

[13] A. Salis, M. Monduzzi, Not only pH. Specific buffer effects in biological systems, Current Opinion in Colloid and Interface Science 23 (2016) 1–9.

[14] K. Mizutani, Y. Chen, H. Yamashita, M. Hirose, S. Aibara, Thermostabilization of ovotransferrin by anions for pasteurization of liquid egg white, Bioscience Biotechnology and Biochemistry 70 (2006) 1839–1845.

[15] L. C. De Lencastre Novaes, P. G. Mazzola, A. Pessoa, T. C. V. Penna, Citrate and phosphate influence on green fluorescent protein thermal stability, Biotechnology Progress 27 (2011) 269–272.

[16] T. M. Mezzasalma, J. K. Kranz, W. Chan, G. T. Struble, C. Schalk-Hihi, I. C. Deckman, B. A. Springer, M. J. Todd, Enhancing recombinant protein quality and yield by protein stability profiling, Journal of Biomolecular Screening 12 (2007) 418–428.

[17] D. Mcphail, C. Holt, Effect of anions on the denaturation and aggregation of -Lactoglobulin as measured by differential scanning microcalorimetry, International Journal of Food Science and Technology 34 (1999) 477–481.

[18] D. Bilaničová, A. Salis, B. W. Ninham, M. Monduzzi, Specific anion effects on enzymatic activity in nonaqueous media, Journal of Physical Chemistry B 112 (2008) 12066–12072.

[19] X. M. Cao, Y. Tian, Z. Y. Wang, Y. W. Liu, C. X. Wang, Effects of protein and phosphate buffer concentrations on thermal denaturation of lysozyme analyzed by isoconversional method, Bioengineered 7 (2016) 235–240.

[20] L. Haifeng, L. Yuwen, C. Xiaomin, W. Zhiyong, W. Cunxin, Effects of sodium phosphate buffer on horseradish peroxidase thermal stability, Journal of Thermal Analysis and Calorimetry 93 (2008) 569–574.

[21] H. Tomizawa, H. Yamada, Y. Hashimoto, T. Imoto, Stabilization of lysozyme against irreversible inactivation by alterations of the Asp-Gly

sequences, Protein Engineering, Design and Selection 8 (1995) 1023–1028.

[22] H. I. Okur, J. Hladílková, K. B. Rembert, Y. Cho, J. Heyda, J. Dzubiella, P. S. Cremer, P. Jungwirth, Beyond the Hofmeister Series: Ion-Specific Effects on Proteins and Their Biological Functions 121 (2017) 1997–2014.

[23] J. Paterová, K. B. Rembert, J. Heyda, Y. Kurra, H. I. Okur, W. R. Liu, C. Hilty, P. S. Cremer, P. Jungwirth, Reversal of the hofmeister series: Specific ion effects on peptides, Journal of Physical Chemistry B 117 (2013) 8150–8158.

[24] P. Bruździak, A. Panuszko, E. Kaczkowska, B. Piotrowski, A. Daghir, S. Demkowicz, J. Stangret, Taurine as a water structure breaker and protein stabilizer, Amino Acids 50 (2018) 125–140.

[25] M. Śmiechowski, E. Gojło, J. Stangret, Systematic study of hydration patterns of phosphoric(V) Acid and its mono-, di-, and tripotassium salts in aqueous solution, Journal of Physical Chemistry B 113 (2009) 7650–7661.

[26] W. W. Rudolph, Raman- and infrared-spectroscopic investigations of dilute aqueous phosphoric acid solutions, Dalton Transactions 39 (2010) 9642.

[27] A. B. Pribil, T. S. Hofer, B. R. Randolf, B. M. Rode, Structure and dynamics of phosphate ion in aqueous solution: An ab initio QMCF MD study, Journal of Computational Chemistry 29 (2008) 2330–2334.

[28] W. W. Rudolph, G. Irmer, Raman and infrared spectroscopic investigations on aqueous alkali metal phosphate solutions and density functional theory calculations of phosphate-water clusters, Applied Spectroscopy 61 (2007) 1312–1327.

[29] C. C. Pye, W. W. Rudolph, An ab initio, infrared, and Raman investigation of phosphate ion hydration, Journal of Physical Chemistry A 107 (2003) 8746–8755.

[30] P. E. Mason, J. M. Cruickshank, G. W. Neilson, P. Buchanan, Neutron scattering studies on the hydration of phosphate ions in aqueous solutions of K_3PO_4, K_2HPO_4 and KH_2PO_4, Physical Chemistry Chemical Physics 5 (2003) 4686.

[31] V. K. Yadav, A. Chandra, First-Principles Simulation Study of Vibrational Spectral Diffusion and Hydrogen Bond Fluctuations in Aqueous Solution of N -Methylacetamide, Journal of Physical Chemistry B 119 (2015) 9858–9867.

[32] V. Vasylyeva, S. K. Nayak, G. Terraneo, G. Cavallo, P. Metrangolo, G. Resnati, Orthogonal halogen and hydrogen bonds involving a peptide bond model, CrystEngComm 16 (2014) 8102–8105.

[33] J. Heyda, J. C. Vincent, D. J. Tobias, J. Dzubiella, P. Jungwirth, Ion specificity at the peptide bond: Molecular dynamics simulations of N-methylacetamide in aqueous salt solutions, Journal of Physical Chemistry B 114 (2010) 1213–1220.

[34] L. C. Mayne, B. Hudson, Resonance Raman Spectroscopy of N-Methylacetamide: Overtones and Combinations of the C-N Stretch (Amide II') and Effect of Solvation on the C=O Stretch (Amide I) Intensity, The Journal of Physical Chemistry 95 (1991) 2962–2967.

[35] W. L. Jorgensen, J. Gao, Cis-Trans Energy Difference for the Peptide Bond in the Gas Phase and in Aqueous Solution, Journal of the American Chemical Society 110 (1988) 4212–4216.

[36] J. M. Dudik, C. R. Johnson, S. A. Asher, UV resonance Raman studies of acetone, acetamide, and N-methylacetamide: Models for the peptide bond, Journal of Physical Chemistry 89 (1985) 3805–3814.

[37] H. Yu, C. L. Mazzanti, T. W. Whitfield, R. E. Koeppe, O. S. Andersen, B. Roux, A Combined Experimental and Theoretical Study of Ion Solvation in Liquid N-Methylacetamide, Journal of the American Chemical Society 132 (2010) 10847–10856.

[38] T. Takekiyo, Y. Yoshimura, Y. Ikeji, N. Hatano, T. Koizumi, Raman spectroscopic study on the coordination behavior of rare earth ions in N-methylacetamide, J Phys Chem B 112 (2008) 13355–13358.

[39] A. A. Dyshin, O. V. Eliseeva, M. G. Kiselev, Density and Viscosity of N -MethylacetamideCalcium Chloride Mixtures over the Temperature Range from 308.15 to 328.15 K at Atmospheric Pressure, Journal of Chemical & Engineering Data 62 (2017) 4128–4132.

[40] T. Forsting, H. C. Gottschalk, B. Hartwig, M. Mons, M. A. Suhm, Cor-

recting the record: the dimers and trimers of trans-N-methylacetamide, Phys. Chem. Chem. Phys. 19 (2017) 10727–10737.

[41] M. Albrecht, C. A. Rice, M. A. Suhm, Elementary peptide motifs in the gas phase: FTIR aggregation study of formamide, acetamide, N-methylformamide, and N-methylacetamide, Journal of Physical Chemistry A 112 (2008) 7530–7542.

[42] P. A. Cazade, T. Bereau, M. Meuwly, Computational two-dimensional infrared spectroscopy without maps: N-methylacetamide in water, Journal of Physical Chemistry B 118 (2014) 8135–8147.

[43] J. Jeon, M. Cho, Direct quantum mechanical/molecular mechanical simulations of two-dimensional vibrational responses: N-methylacetamide in water, New Journal of Physics 12 (2010) 065001.

[44] K. Kwac, M. Cho, Hydrogen bonding dynamics and two-dimensional vibrational spectroscopy: N-methylacetamide in liquid methanol, Journal of Raman Spectroscopy 36 (2005) 326–336.

[45] H. Huang, S. Malkov, M. Coleman, P. Painter, Two-dimensional correlation infrared spectroscopic study of N-methylacetamide as a function of temperature, J Phys Chem A 107 (2003) 7697–7703.

[46] G. Eaton, M. C. R. Symons, P. P. Rastogi, Spectroscopic studies of the solvation of amides with NH groups. Part 1.The carbonyl group, Journal of the Chemical Society, Faraday Transactions 1: Physical Chemistry in Condensed Phases 85 (1989) 3257.

[47] E. Salamatova, A. V. Cunha, R. Bloem, S. J. Roeters, S. Woutersen, T. L. C. Jansen, M. S. Pshenichnikov, Hydrophobic Collapse in N - MethylacetamideWater Mixtures, The Journal of Physical Chemistry A 122 (2018) acs.jpca.8b00276.

[48] T. W. Whitfield, G. J. Martyna, S. Allison, S. P. Bates, H. Vass, J. Crain, Structure and Hydrogen Bonding in Neat N-Methylacetamide : Classical Molecular Dynamics and Raman Spectroscopy Studies of a Liquid of Peptidic Fragments, The Journal of Physical Chemistry B 110 (2006) 3624–3637.

[49] A. Chand, S. Chowdhuri, Effects of dimethyl sulfoxide on the hydrogen bonding structure and dynamics of aqueous N-methylacetamide solution, Journal of Chemical Sciences 128 (2016) 991–1001.

[50] S. K. Pattanayak, P. Chettiyankandy, S. Chowdhuri, Effects of co-solutes on the hydrogen bonding structure and dynamics in aqueous N-methylacetamide solution: A molecular dynamics simulations study, Molecular Physics 112 (2014) 2906–2919.

[51] S. Paul, S. Paul, Influence of temperature on the solvation of N-methylacetamide in aqueous trehalose solution: A molecular dynamics simulation study, Journal of Molecular Liquids 211 (2015) 986–999.

[52] A. Panuszko, E. Gojło, J. Zielkiewicz, M. Śmiechowski, J. Krakowiak, J. Stangret, Hydration of simple amides. FTIR Spectra of HDO and theoretical studies, Journal of Physical Chemistry B 112 (2008) 2483–2493.

[53] M. Śmiechowski, J. Stangret, Vibrational spectroscopy of semiheavy water (HDO) as a probe of solute hydration, Pure and Applied Chemistry 82 (2010).

[54] J. Stangret, T. Gampe, Ionic hydration behavior derived from infrared spectra in HDO, Journal of Physical Chemistry A 106 (2002) 5393–5402.

[55] P. Bruździak, P. W. Rakowska, J. Stangret, Chemometric method of spectra analysis leading to isolation of lysozyme and CtDNA spectra affected by osmolytes, Applied Spectroscopy 66 (2012) 1302–1310.

[56] P. Bruździak, A. Panuszko, J. Stangret, Chemometric determination of solute-affected solvent vibrational spectra as a superior way of information extraction on solute solvation phenomena, Vibrational Spectroscopy 54 (2010) 65–71.

[57] J. Stangret, Solute-Affected Vibrational Spectra of Water in $Ca(ClO_4)_2$ Aqueous Solutions, Spectroscopy Letters 21 (1988) 369–381.

[58] Y. Zhao, D. G. Truhlar, Y. Zhao, D. G. Truhlar, The M06 suite of density functionals for main group thermochemistry, thermochemical kinetics, noncovalent interactions, excited states, and transition elements: Two new functionals and systematic testing of four M06-class functionals and 12 other function, Theoretical Chemistry Accounts 120 (2008) 215–241.

[59] R. A. Kendall, T. H. Dunning, R. J. Harrison, Electron affinities of the first-row atoms revisited. Systematic basis sets and wave functions, The Journal of Chemical Physics 96 (1992) 6796–6806.

[60] M. Cossi, N. Rega, G. Scalmani, V. Barone, Energies, structures, and electronic properties of molecules in solution with the C-PCM solvation model, Journal of Computational Chemistry 24 (2003) 669–681.

[61] V. Barone, M. Cossi, Quantum calculation of molecular energies and energy gradients in solution by a conductor solvent model, Journal of Physical Chemistry A 102 (1998) 1995–2001.

[62] S. F. Boys, F. Bernardi, The calculation of small molecular interactions by the differences of separate total energies. Some procedures with reduced errors, Molecular Physics 19 (1970) 553–566.

[63] Y. K. Kang, H. S. Park, Internal rotation about the C-N bond of amides, Journal of Molecular Structure: THEOCHEM 676 (2004) 171–176.

[64] Y. K. Kang, Ab initio MO and density functional studies on trans and cis conformers of N-methylacetamide, Journal of Molecular Structure: THEOCHEM 546 (2001) 183–193.

[65] A. Radzicka, L. Pedersen, R. Wolfenden, Influences of Solvent Water on Protein Folding: Free Energies of Solvation of Cis and Trans Peptides Are Nearly Identical, Biochemistry 27 (1988) 4538–4541.

[66] R. F. W. Bader, A Quantum Theory of Molecular Structure and Its Applications, Chemical Reviews 91 (1991) 893–928.

[67] E. Espinosa, E. Molins, C. Lecomte, Hydrogen bond strengths revealed by topological analyses of experimentally observed electron densities, Chemical Physics Letters 285 (1998) 170–173.

[68] M. J. Frisch, G. W. Trucks, H. B. Schlegel, G. E. Scuseria, M. A. Robb, J. R. Cheeseman, G. Scalmani, V. Barone, B. Mennucci, G. A. Petersson, H. Nakatsuji, M. Caricato, X. Li, H. P. Hratchian, A. F. Izmaylov, J. Bloino, G. Zheng, J. L. Sonnenberg, M. Hada, M. Ehara, K. Toyota, R. Fukuda, J. Hasegawa, M. Ishida, T. Nakajima, Y. Honda, O. Kitao, H. Nakai, T. Vreven, J. A. Montgomery Jr., J. E. Peralta, F. Ogliaro, M. Bearpark, J. J. Heyd, E. Brothers, K. N. Kudin, V. N. Staroverov, R. Kobayashi, J. Normand, K. Raghavachari, A. Rendell, J. C. Burant, S. S. Iyengar, J. Tomasi, M. Cossi, N. Rega, J. M. Millam, M. Klene, J. E. Knox, J. B. Cross, V. Bakken, C. Adamo, J. Jaramillo, R. Gomperts, R. E. Stratmann, O. Yazyev, A. J. Austin, R. Cammi, C. Pomelli, J. W. Ochterski, R. L. Martin, K. Morokuma, V. G. Zakrzewski, G. A. Voth, P. Salvador, J. J. Dannenberg, S. Dapprich, A. D. Daniels, Ö. Farkas, J. B. Foresman, J. V. Ortiz, J. Cioslowski, D. J. Fox, Gaussian 09, Revision D.01, 2009.

[69] M. D. Hanwell, D. E. Curtis, D. C. Lonie, T. Vandermeerschd, E. Zurek, G. R. Hutchison, Avogadro: An advanced semantic chemical editor, visualization, and analysis platform, Journal of Cheminformatics 4 (2012) 17.

[70] T. Lu, F. Chen, Multiwfn: A multifunctional wavefunction analyzer, Journal of Computational Chemistry 33 (2012) 580–592.

[71] K. J. Schostack, E. R. Malinowski, Preferred set selection by iterative key set factor analysis, Chemometrics and Intelligent Laboratory Systems 6 (1989) 21–29.

[72] E. R. Malinowski, Obtaining the key set of typical vectors by factor analysis and subsequent isolation of component spectra, Analytica Chimica Acta 134 (1982) 129–137.

[73] M. Akiyama, Study on hydration enthalpy of n-methylacetamide in water, Spectrochimica Acta Part A: Molecular and Biomolecular Spectroscopy 58 (2002) 1943 – 1950.

[74] I. M. Klotz, J. S. Franzen, Hydrogen bonds between model peptide groups in solution, Journal of the American Chemical Society 84 (1962) 3461–3466.

[75] P. Persson, N. Nilsson, S. Sjöberg, Structure and bonding of orthophosphate ions at the iron oxide-aqueous interface, Journal of Colloid and Interface Science 177 (1996) 263–275.

[76] E. M. Fatila, M. Pink, E. B. Twum, J. A. Karty, A. H. Flood, Phosphatephosphate oligomerization drives higher order co-assemblies with stacks of cyanostar macrocycles, Chemical Science (2018).

[77] J. M. Shaver, K. A. Christensen, J. A. Pezzuti, M. D. Morris, Structure of dihydrogen phosphate ion aggregates by Raman-monitored serial dilution, Applied Spectroscopy 52 (1998) 259–264.

[78] F. Rull, A. Del Valle, F. Sobron, S. Veintemillas, Raman study of phosphate dimerization in aqueous KH_2PO_4 solutions using a selfdeconvolution method, Journal of Raman Spectroscopy 20 (1989) 625–631.

[79] P. Bruździak, B. Adamczak, E. Kaczkowska, J. Czub, J. Stangret, Are stabilizing osmolytes preferentially excluded from the protein surface?

FTIR and MD studies, Physical Chemistry & Chemical Physics 17 (2015) 23155–23164.

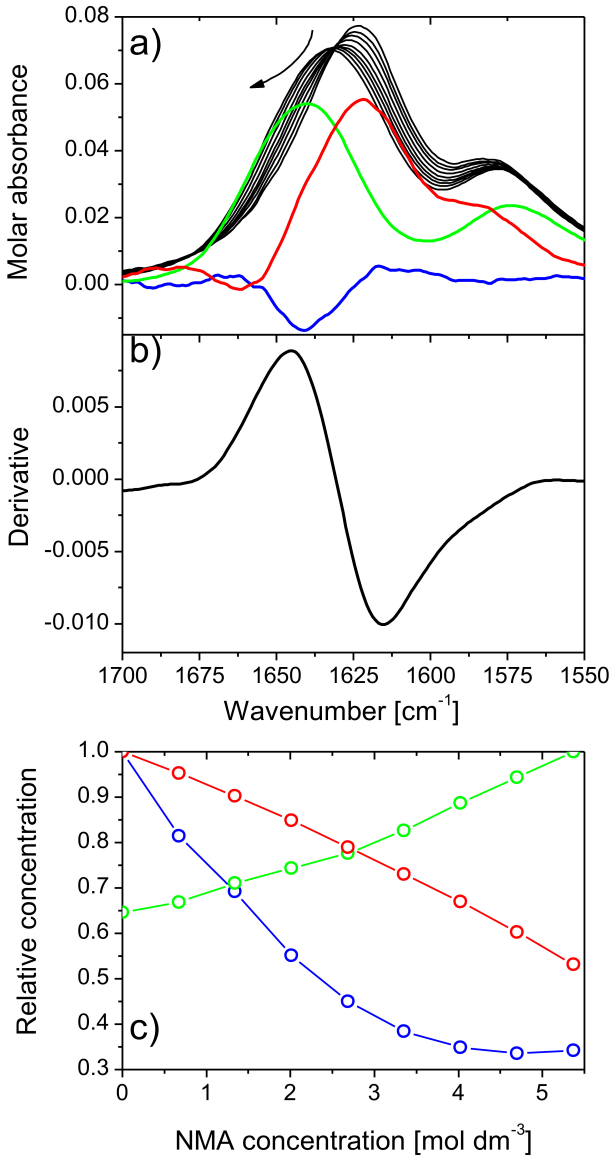

Figure 1: a) Changes in the band shape of C=O stretching and N–H bending vibrations of NMA molecule caused by its concentration increase; colors indicate first three principal factors. b) The difference derivative spectrum isolated from the series, with the band shape characteristic for a shift of a band towards higher wavenumbers. c) Relative concentrations of principal factors (colors correspond to those in Figure a).

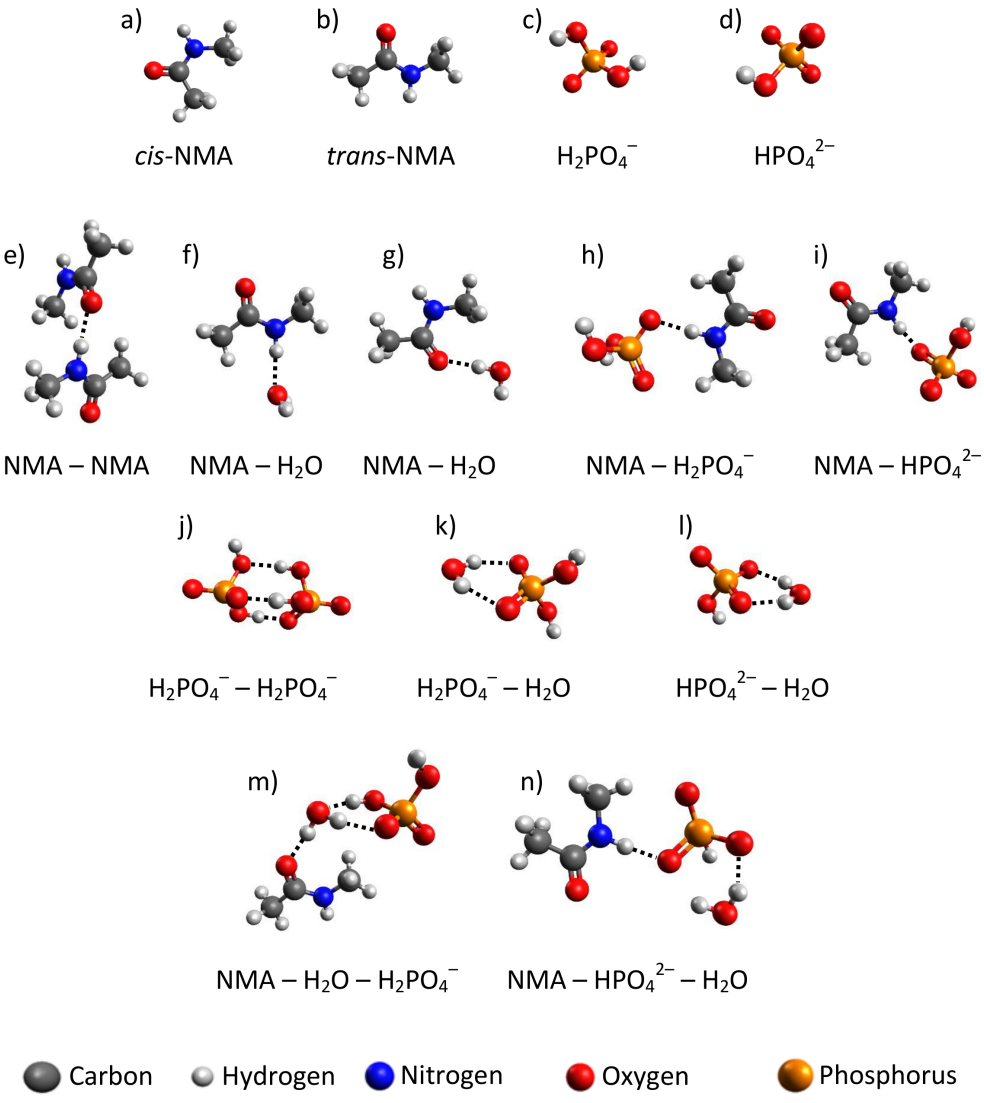

Figure 2: Optimized structures of NMA, $H_2PO_4^-$, HPO_4^{2-}, and their complexes. Names of these structures are the same as in Tables 1 and 2.

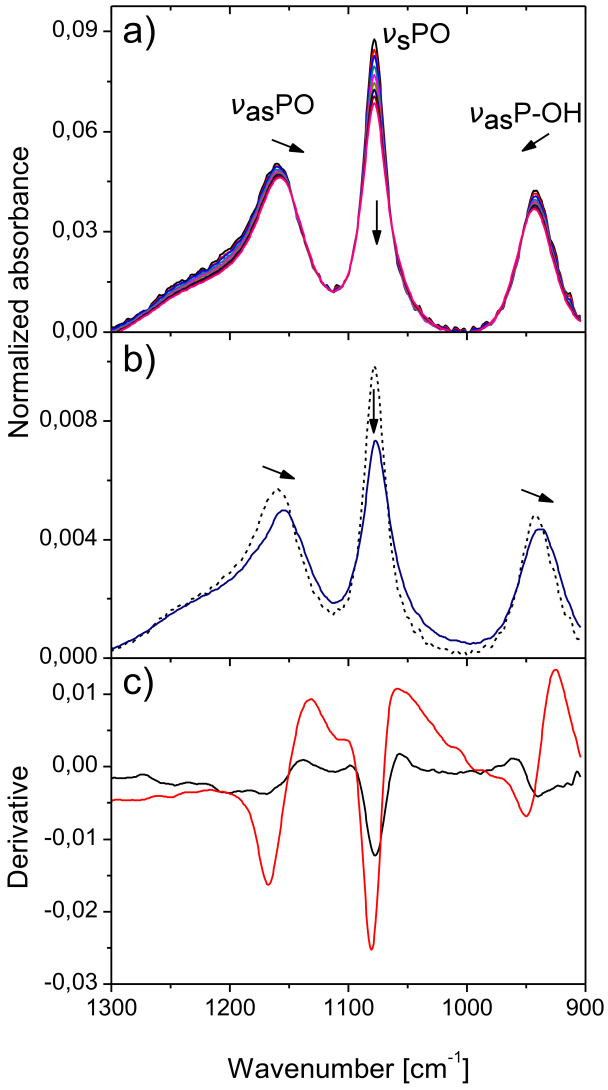

Figure 3: a) Changes in the band shape of PO vibration region caused only by the change in $H_2PO_4^-$ ion concentration. b) the bulk (dashed) spectrum of phosphate ion and its mean spectrum affected by the presence of NMA. Arrows indicate the direction of main differences. c) The derivative D isolated from the series in figure a) (black), and the mean difference affected spectrum isolated from series of NMA-affected spectra of $H_2PO_4^-$ (red). The meaning of the derivative is explained in paragraph 2.2.2.

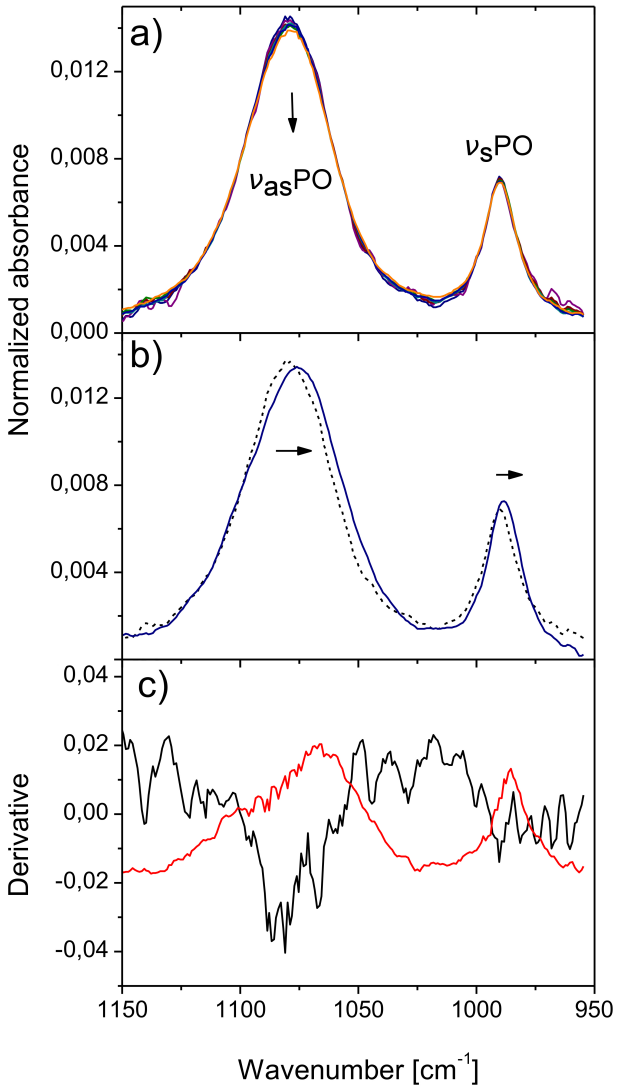

Figure 4: a) Changes in the band shape of PO vibration region caused only by the change in HPO_4^{2-} ion concentration. b) the bulk (dashed) spectrum of phosphate ion and its mean spectrum affected by the presence of NMA. Arrows indicate the direction of main differences. c) The derivative D isolated from the series in figure a) (black), and the mean difference affected spectrum isolated from series of NMA-affected spectra of HPO_4^{2-} (red). The meaning of the derivative is explained in paragraph 2.2.2.

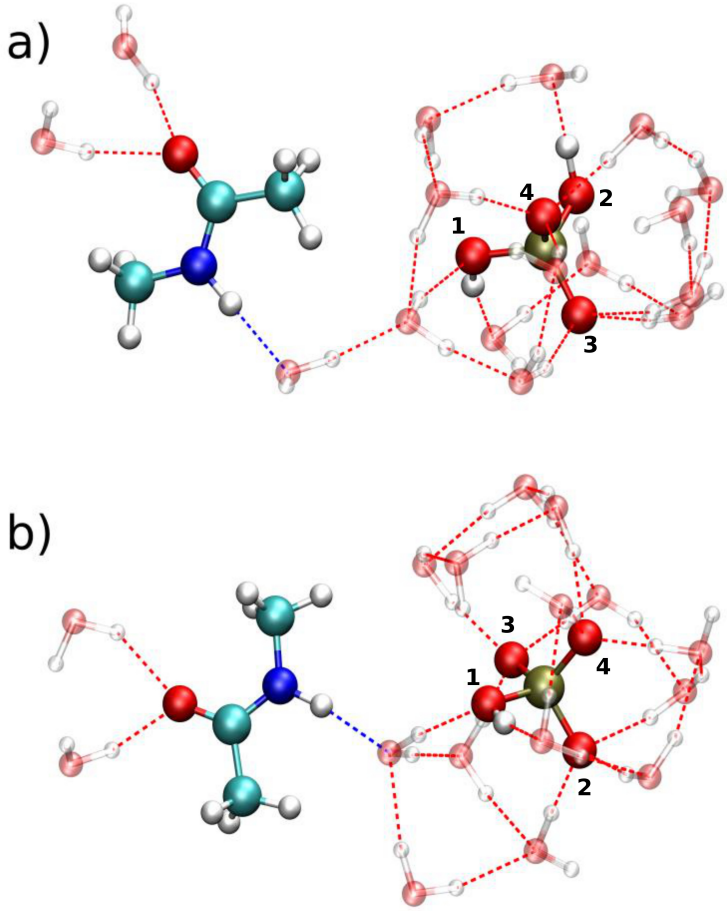

Figure 5: Selected optimized geometries of NMA-phosphate ion hydrated complexes. a) $H_2PO_4^-$–based system. b) HPO_4^{2-}–based system.

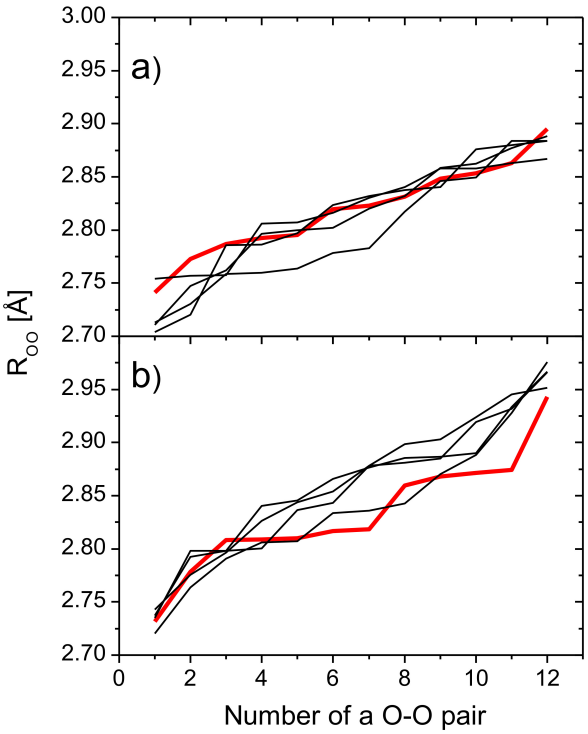

Figure 6: The distribution of oxygen-oxygen distances in the hydration layer of a) $H_2PO_4^-$ and b) HPO_4^{2-} systems. Only twelve shortest pair distances are presented. Red lines indicate systems consisting only of phosphate ion and hydration water. Black lines represents the distribution for systems including NMA molecule with its three water molecules, corresponding to four different starting NMA-ion orientations.